ARTICLE

J. Cent. South Univ. (2019) 26: 1050−1064
DOI: https://doi.org/10.1007/s11771-019-4070-2

Springer

Effects of reinforced nanofluid with nanoparticles on cutting tool wear morphology

Seyed Hasan MUSAVI, Behnam DAVOODI, Seyed Ali NIKNAM

School of Mechanical Engineering, Iran University of Science and Technology, Tehran 16846-13114, Iran

Abstract: Superalloys are grouped as hard-to-cut materials with relatively poor machinability. Tool wear is considered one of the main machinability attributes in machining superalloys. Although numerous works have been reported on factors governing tool life in machining superalloys, no study was found on the effect of nanoparticles stability on nanofluid performance and consequently resulted tool wear morphologies. In the present work, the nanoparticles were reinforced by means of improving the stability of the base fluid. To that accomplished, the surface active agent (surfactant) was added to the base cutting fluid as a reinforcing element. The effects of new lubricant on the tool wear morphology of A286 works parts were assessed.

Key words: nanofluid; surface active agent (surfactant); nanoparticles dispersion; built-up edge

Cite this article as: Seyed Hasan MUSAVI, Behnam DAVOODI, Seyed Ali NIKNAM. Effects of reinforced nanofluid with nanoparticles on cutting tool wear morphology [J]. Journal of Central South University, 2019, 26(5): 1050–1064. DOI: https://doi.org/10.1007/s11771-019-4070-2.

1 Introduction

Superalloys have high toughness, high strength, corrosion resistance, abrasion resistance, and excellent creep-rupture strength at high temperatures. They are widely used in strategic manufacturing sectors, including aerospace industry, nuclear, shipbuilding, and power plant, etc. In addition, A286 is used in jet engines, superchargers and various high temperature applications such as turbine wheels and blades, frames, casings, afterburners parts and fasteners. According to unique properties aforementioned, superalloys are classified as difficult-to-cut materials which exhibit poor machinability. Features such as low thermal conductivity, high toughness as well as hard abrasive particles lead to catastrophic tool wear when machining superalloys [1–8]. Furthermore, three other main categories are attributed to be difficult to cut materials, including materials with high toughness (e.g., nickels and titanium alloys), high hardness (e.g., D2 tool steel with high-carbon and high-chromium), and non-homogeneous morphology (e.g., composites). Superalloys are the first division aforementioned [9].

The very low thermal conductivity of superalloys is the main reason of a sudden rise of cutting temperature. On the other hand, high strength of these metals, especially at high temperatures, increases the induced compressive stress on the tool rake face. The first phenomenon raises the possibility of adhesion wear, and the later may lead to abrasion on the tool face. Also, the presence of γ intermetallic phase drastically increases the strength of superalloys. Due to its ordered nature and high coherency with the γ matrix, notch wear and consequently tool failure may occur. As a result, those cutting tools used in machining superalloys are subjected to various tool wear

Received date: 2018-09-15; **Accepted date:** 2018-12-13
Corresponding author: Behnam DAVOODI, PhD, Associate Professor; Tel: +98-21-73228911; E-mail: bdavoodi@iust.ac.ir; ORCID: 0000-0001-7102-3291

modes and limited tool life. Because of their extensive applications in different industrial sectors, it is beneficial to propose innovative strategies to enhance the useful life of those cutting tools used in machining superalloys [10–15].

The effects of different cooling-lubrication strategies on tool wear reduction have been studied in a large extent [14–21]. POLVOROSA et al [14] studied the effects of different coolant based pressures such as high-pressure cooling on the tool wear when turning Inconel 718 and Waspaloy. FANG et al [16] presented the cooling channels constructed on the inserts under high-pressure jet coolant when turning of Inconel 718. CANTERO et al [17] evaluated the modes of tool wear in finishing of Inconel 718 work parts under different cooling-lubrication methods. HOIER et al [18] supplied the high-pressure coolant to improve the flank wear of WC-Co tools when turning Inconel 718. LIMA et al [19] studied the modes of wear in the ceramic-based cutting tools in machining Inconel 751 when both argon and oxygen were used as the cooling gas. BEHERA et al [20] presented a comparative study of different machining and lubrications modes such as high-pressure jet, cryogenic cooling, MQL and nano-based MQL to evaluate the tool wear during turning of Ni-based superalloys. TAZEHKANDI et al [21] investigated the use of liquid nitrogen and the modes of delivering biodegradable vegetable fluid towards reducing the tool wear and cutting forces in turning Inconel 740.

The use of coated carbide tools in machining superalloys has been reported in Refs. [22–26]. It was observed that lower friction coefficient between the tool and work part and consequently lower cutting temperature is expected when the coated cutting tool is used. GRZESIK et al [22] studied the effect of PVD-TiAlN, AlTiN coated carbide grades with the dissimilar percentage of Ti and Al compounds on the tool wear in turning Inconel 718. MARTINEZ et al [23] evaluated the effects of coating on the flank wear when turning Inconel 718. Also, the effects of coating layer loss on the variation of wear rate in turning process were determined. CALISKAN et al [24] investigated the influence of CN/TiAlN coating on the tool wear, cutting forces, surface quality and chip morphology in machining titanium alloy. NIAKI et al [25] presented a broad study on the influences of tool wear on surface quality, residual stresses and dimensional integrity in machining of Inconel 718 when using TiAlN coated carbide tools. KOSEKI et al [26] compared the performance of TiN coating inserts using CVD and PVD operations during uninterrupted cutting of nickel-based alloys. CHEN et al [7] evaluated the wear morphology of PVD TiN-based coating tools in turning of nickel-based and titanium-based alloys by different cooling-lubrication methods.

Several treatment methods, such as constructing textured surfaces on the insert, were conducted to reduce the tool-chip contact. SUGIHARA et al [27] established a novel CBN cutting tool with a textured flank face. The effects of textured surfaces on the tool wear were assessed when turning Inconel 718. FANG et al [28] studied the effects of micro-texture of the tool flank face on the cooling strength and consequently on the tool wear morphology and size. Orthogonal turning was performed on Inconel 718 when using high-pressure jet coolant. The last few decades have been inspired with a new class of fluid, so-called nanofluids, which include nanoparticles (nanometer-sized of solid particles). Nanofluids which were initially presented by CHOI et al [29] seem to generate a high rate of heat transfer as compared to conventional cutting fluids. Nanoparticles with low volume fraction are added into cutting fluid. Nanoparticles are the additives in nanofluids, and they play the main role in increasing the lubrication and thermal transport properties of nanofluids [30].

It has been observed that using nanofluid could provide good cutting conditions and consequently reduced tool wear is expected [31–34]. CHETAN et al [31] evaluated the effects of nanofluids on the tool wear and cutting forces during MQL turning of Nimonic 90 alloy. Limited studies were conducted to assess the effects of nanofluids on tool wear reduction when machining superalloys. GUPTA et al [32] optimized the cutting forces, tool wear, cutting temperature and surface finish during MQL turning of titanium alloy when using different nanofluids. PADMINI et al [33] investigated the effect of nanofluid as a potential cutting fluid in turning of steels. The research work presented in Ref. [33] mainly focused on evaluating the effects of vegetable-based nanofluid on the tool wear, cutting forces, surface roughness, and tooltip

temperature during turning of AISI1040 steel. It was exhibited that as compared to dry cutting tests, the tool wear was reduced by approximately 44% when MoS_2-based nanofluid was used. NAJIHA et al [34] examined the tool wear mechanisms in machining aluminum alloy under different operational conditions. The water-based nanofluid (nano-TiO_2) was used as the cutting fluid. It was observed that the adhesion is the main wear mode that can be significantly optimized when nanofluid was used.

As mentioned earlier, limited studies are available on machining A286 iron-based superalloy. On the other hand, no work was found on evaluating the effects of nanoparticles stability on nanofluid performance and consequently on machinability attributes when machining A286 superalloy. In the present work, the surface active agent was used to increase the stability of nanoparticles in the base cutting fluid, and its effect has been studied on the tool wear morphology in MQL turning operations with nanofluid without surfactant (N.F), nanofluid with surfactant (N.F.S) and conventional cutting fluid (C.F).

2 Materials and equipment

2.1 Work part and cutting tool materials

Orthogonal cutting tests were performed on the cylindrical block of the A286 superalloy. The chemical compositions of work part in mass fraction (%) are as follows: Ni 25, Mo 1.2, C 0.05, S 0.025, V 0.2, Al 0.35, Mn 2, Ti 2.1, Si 1, Cr 14, Fe base. Table 1 presents mechanical properties, cutting parameters of A286 superalloy and part geometry used in this study. The cemented SECO carbide insert (SNMG 120404- GC1105) was used in all cutting tests. It should be underlined that in order to maintain the repeatability, a new insert was used in each cutting test. The applied insert has high wear resistance and good toughness which is considered an ideal candidate for machining superalloys.

The value of surface roughness was recorded using a TR200 profilometer. In each test, five different points parallel to the feed rate direction were measured, and the average value was recorded for experimental analysis.

2.2 Nanofluid

Copper-oxide and silicon-oxide nanoparticles were used by means of suspension in the cutting fluid. The mechanical properties of the nanoparticle employed in this work are shown in Table 2. In order to produce a dispersed solution of nanofluid with high-stability of the nanoparticles, the surfactant was used as an additive. Surfactants have different categories which are selected with regard to the solvent compositions. According to the polar solvent of cutting fluid used in this study, the sodium dodecyl sulfate (SDS) was used as the proper surfactant. The surfactant with 10% volume fraction of total nanoparticles was added to the base cutting fluid. Prepared nanofluid from nanoparticles and surfactant was placed in an ultrasonic bath for an hour to produce a suitable suspension. Figure 1 shows the copper-oxide and silicon-oxide nanoparticles, as well as surfactant used in this study.

Table 1 Specifications of A286 superalloy

Mechanical property						
Elastic modulus/GPa	Thermal conductivity/ ($W \cdot m^{-1} \cdot K^{-1}$)	Density/ ($kg \cdot m^{-3}$)	Melting point/°C	Elongation/ %	Ultimate tensile strength/MPa	Yield strength/MPa
201	15.1	7920	1430	40	620	275
Cutting parameter			Work part geometry			
Cutting speed/ ($m \cdot min^{-1}$)	Feed rate/ ($mm \cdot r^{-1}$)	Depth of cut/mm	Circular cross-section	Diameter/ mm	Length/ mm	Length of machining area/mm
45, 70, 95	0.12, 0.22, 0.32	1		60	130	60

Table 2 Mechanical properties of nanoparticles used

Nanoparticle	Density/($g \cdot cm^{-3}$)	Melting point/°C	Morphology	Color	Diameter/nm	Purity/%
Silicon oxide	2.2	1600	Spherical	White	20	98
Copper oxide	6.31	1200	Spherical	Black	40	99

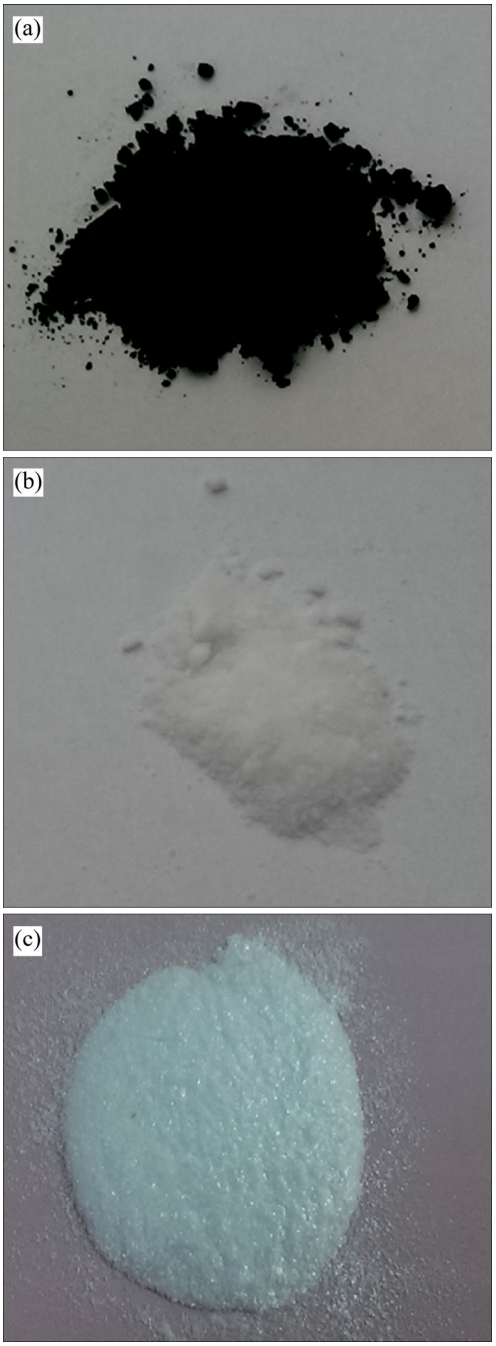

Figure 1 Nanoparticles and surfactant: (a) Copper-oxide nanoparticles; (b) Silicon-oxide nanoparticles; (c) Surfactant (SDS)

2.3 Cooling-lubrication method

As noted earlier, the MQL system was used to supply the cutting fluid to the cutting zone. The presented MQL system in this work was designed and manufactured at sustainable manufacturing systems laboratory (SMSL) and the precision and accuracy of the developed machine were confirmed through preliminary experimental tests. Within the MQL system used, the cutting fluid was mixed with compressed air under a specific mechanism, and their mixture is delivered to the cutting zone via nozzles through an indirect embedded path. Under such circumstances, the penetration ability of cutting fluid particles to the cutting zone was significantly improved [4, 20] and better cooling performance is expected. In the present study, the flow rate and injection pressure of cutting fluid were adjusted to 150 cm^3/h and 600 kPa, respectively. Also, in the flood mode, the flow rate was low, and it was set on 1 L/min. Figure 2 shows the experimental setup under both MQL and dry modes.

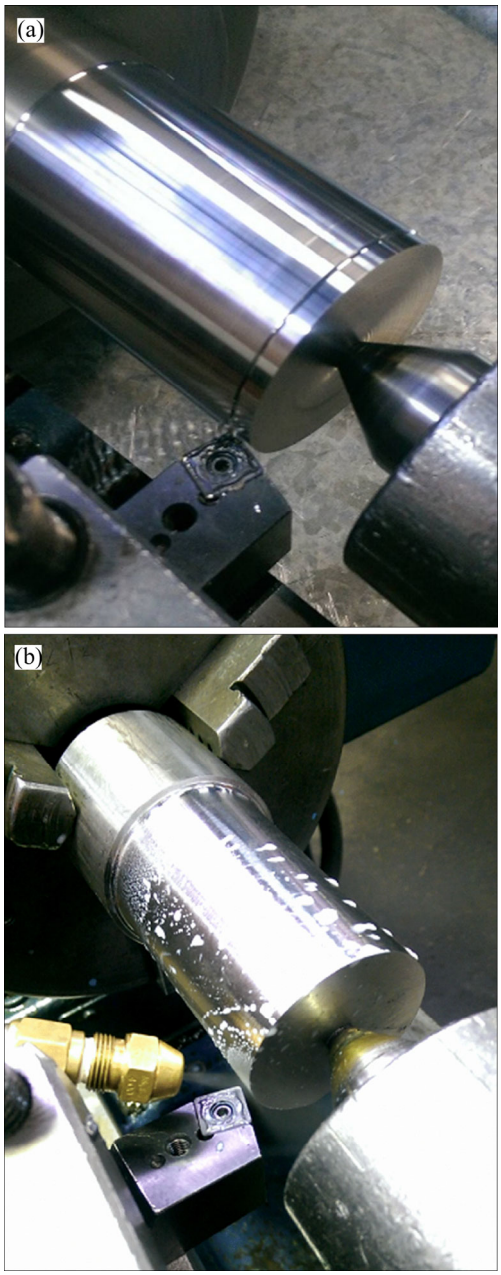

Figure 2 Experimental setup: (a) Dry mode; (b) MQL mode

3 Results and discussion

Tool wear is one of the main machinability index [35–38]. Complementary studies towards better understanding the effects of nanoparticles on machining performance are demanded [36–40]. This may tend to maximize the tool life and finish quality of the products [41]. The main tool wear modes are abrasion, adhesion, notch, diffusion, chemical erosion, etc. [42]. Abrasion and adhesion mechanisms are the main wear modes that appear during machining high toughness materials such as superalloys [43]. The adhesion mechanism can be formed within a vast range of cutting temperature. The built-up edge (BUE) and built-up layer (BUL) are the main consequences of the adhesion.

Figure 3 shows the SEM image of the tool rake face under MQL based conventional cutting fluid. According to Figure 3, the typical tool wear modes appear on the rake face when conventional cutting fluids are used. Referring to high toughness and low thermal conductivity as the unique properties of A286 superalloy, the cutting temperature quickly increases, and the chip particles attach to the tool rake face. After a while, these materials detach, and two phenomenon occur as follows:

1) When cutting tool temperature is increased, the thermal softening occurs, and the removed materials squeeze between tool flank face and machined surface [44] (Figure 4).

2) At the second mode, due to high stiffness of the welded zone in the tool face, several layers of the tool rake face are removed with adhered materials [42]. Under such circumstances, a cavity is created on the cutting tool surface. Consequently, the tool strength reduces and failure may occur. These defects are shown in Figure 3 and Figure 4.

Figure 5 shows the SEM image of the tool rake face with more details than presented in Figure 3(a). Figure 5 clearly shows the presence of BUL formation. As shown in Figure 5(a), a flat area can be seen on the top of the BUE. When a BUE forms near the cutting edge, the relative velocity of chip leads to squeezing the attached particles that are enclosed between tool rake face and underneath of the chip surface. Due to severe friction, the high generated heat at this region leads to BUE flow on the tool rake face. Accordingly, the BUL appears. This phenomenon sequentially occurs, and a thick BUL is formed. The flat area on the top of the BUE (Figure 5(a)) indicates the phenomenon aforementioned.

Figure 6 shows the SEM image of the tool rake face when nanofluids with surfactant and conventional cutting fluid were used. According to Figure 6(c), there are three separated areas on the tool rake face when big attached chips were removed from its surface (e.g., Figure 4(a)). The BUE, BUL and breakage regions can be recognized on the tool rake face. Due to the fracture location that is far from the cutting edge, this type of tool wear is thought to be created due to the removal of the attached chips (BUE) from the tool rake face. The white region near the removed layer of the cutting tool in Figure 6(b) shows the removed layer of BUL. Figure 6(a) illustrates the advantage of using nanofluid with surfactant as a perfect cutting fluid which tends to improve the machining performance and tool life. As a result, the enlarged images of tool rake face, as shown in Figure 3(c) and Figure 6(c), consist of BUE that it is the main reason of adhered materials on the work part surface, very similar to the observation made in Figure 4(b). Also, the BUL is the main reason of the

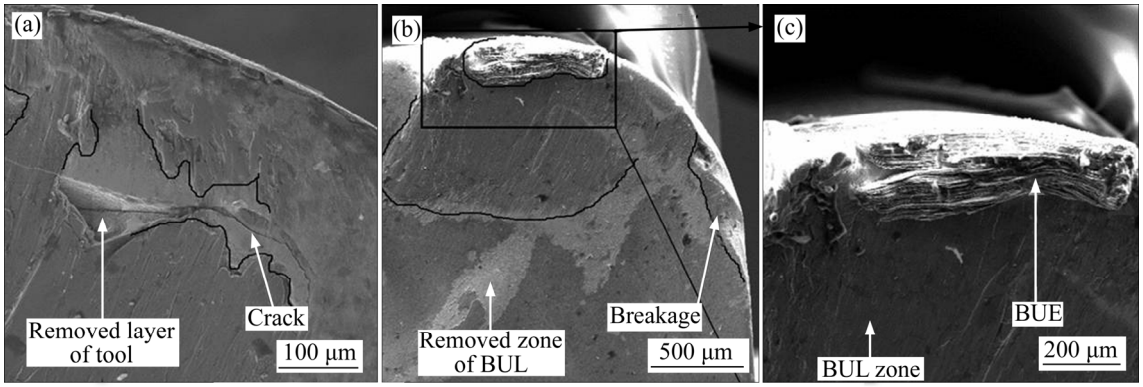

Figure 3 SEM images of tool rake face for MQL based conventional cutting fluid: (a) Breakage on tool rake face; (b) BUL, BUE and edge breakage; (c) Enlarged image

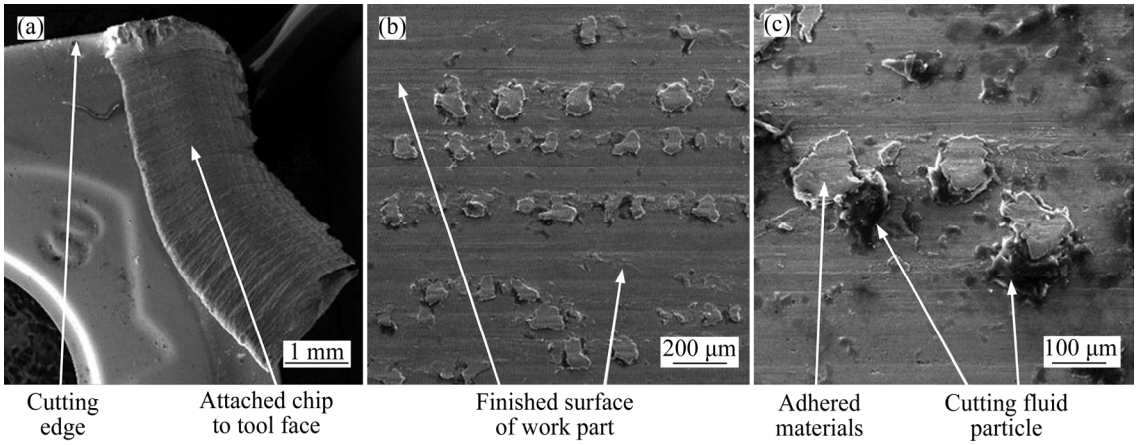

Figure 4 SEM images of tool rake face and work part surface for MQL based conventional cutting fluid: (a) Tool rake face; (b) Adhered materials; (c) Enlarged image

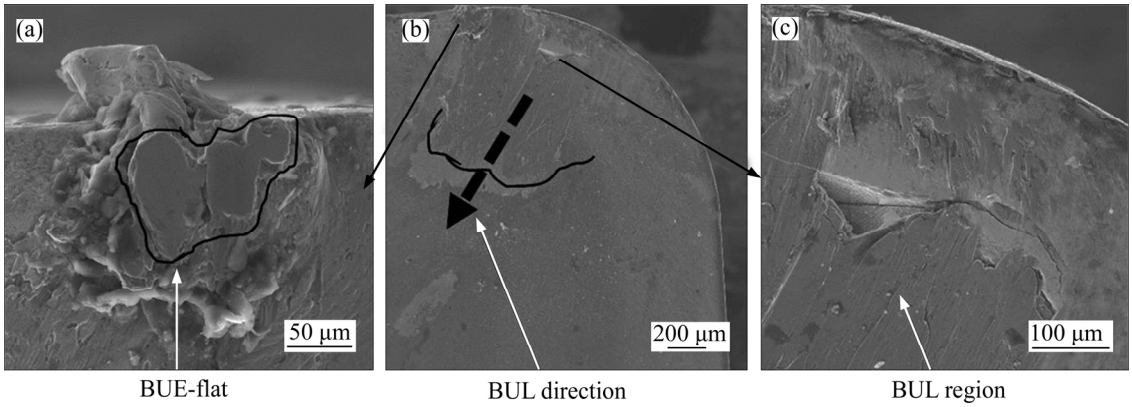

Figure 5 SEM image of BUL formation on tool rake face: (a) Enlarged image of BUE; (b) Tool rake face; (c) Enlarged image of BUL and fracture

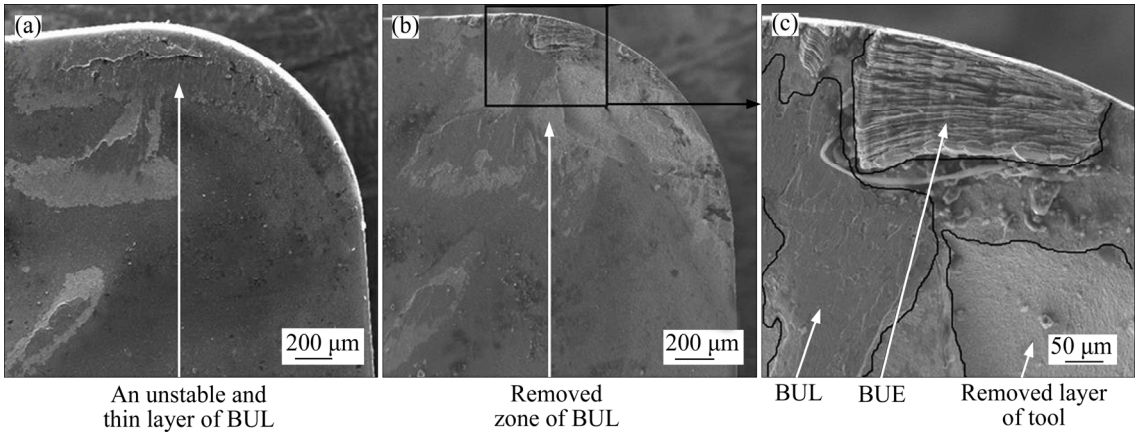

Figure 6 SEM images of tool rake face when turning with nanofluid with surfactant and conventional cutting fluid: (a)Nanofluid+surfactant; (b) Conventional cutting fluid; (c) Enlarged image

removed zone, created on the tool rake face. A similar observation was made in Figure 3(a) and Figure 6(b).

Figure 7 shows the schematic overview of the nanoparticles position at the tool-chip interaction. The reason of tool wear improvement when using nanoparticles can be discussed with Figure 7. During the cutting process, chip with high speed moves on the tool rake face, and these surfaces contact generates a high rate of heat. However, nanoparticles injection led to following four effects as shown in Figure 7 [39]:

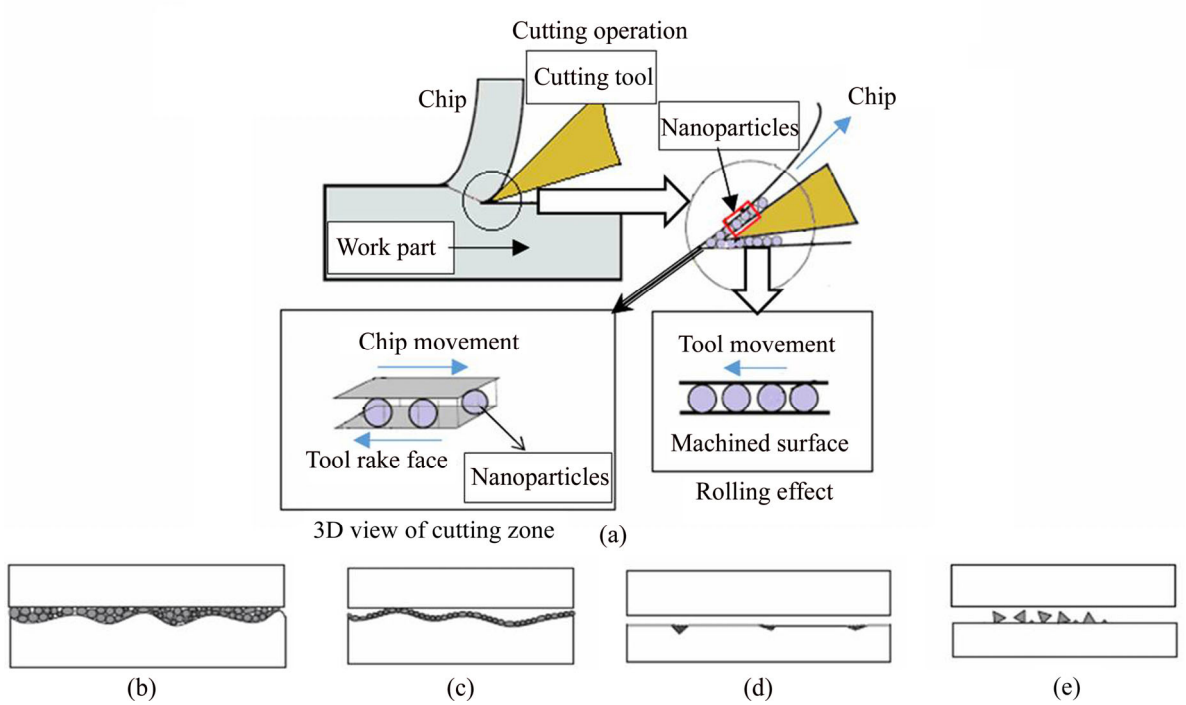

Figure 7 Schematic overview of nanoparticles position at tool-chip interface (a) and 3D view of cutting zone (b)–(e): (b) Rolling effect; (c) Protective film; (d) Mending effect; (e) Polishing effect

3.1 Rolling effect

The high concentration of nanoparticles with fine size and spherical geometry at the tool-chip interface causes the nanoparticles to act as the ball bearings and chip rolls on the tool rake face. Consequently, the direct contact between the metal-metal surfaces (tool-chip) is prevented. By reducing the contact area, the generated heat is reduced, and consequently, the cutting edge maintains sharp, and cutting mechanism proceeds easier. As a result, better tool wear is achieved than that observed by MQL methods without nanoparticles

3.2 Protective film

Due to the high ratio of surface area-to-volume of nanoparticles, these materials tend to attach to each other, and intend to separate out the tool rake face with chip beneath the surface.

3.3 Mending effect

In the presence of several scratches and holes on the work part or tool surface, the nanoparticles inter to these defects due to their small size and consequently provide a flat surface that reduces friction and cutting temperature.

3.4 Polishing effect

Knowing that oxide nanoparticles have high hardness and they are widely used in the machining operation, therefore, sometimes these materials act as an abrasive and polish the surface. Although this factor is not effective as others, it can not be ignored. The main reasons of tool wear improvement from the viewpoint of physical properties of nanoparticles were already stated. The presence of a solid metal phase (nanoparticles) in a liquid phase (cutting fluid) can be attributed to another reason. In fact, metals have better thermal conductivity than liquid. Adding this phase to base cutting fluid increases the heat transfer rate of cutting fluid. As a result, the exchanged heat between the tool and cutting fluid tends to increase.

The chemical analysis was conducted to prove that the adhered materials have the same chemical compositions with the machined parts. Figure 8 represents the EDX examination of indicated points in Figure 4(b). Both EDX examinations indicate that the iron is the main element in their chemical composition. As a result, the substances are iron-based. According to the presence of chrome and nickel elements with high percentage as compared with other elements, it can be expressed that the materials are A286 superalloy. The presence

of carbon and chlorine with high volume fraction is a very interesting point. To better understand this phenomenon, the amounts of carbon and titanium in compositions of A286 superalloy were compared in Table 1 and Figure 8. The amount of titanium (approximately 2.1%) is highly related to carbon (approximately 0.05). However, both EDX examinations as shown in Figure 8 prove that the amount of carbon is more than titanium. This phenomenon can be interpreted by the existence of mineral-based cutting fluid. The cutting fluid used in this work is mineral-based with commercial name of carbon tetrachloride (CCL_4). Because of several layers of lubricant (carbon-based oil) formed on the work part surface, the electron emitted by X-ray spectroscopy device collided with this layer and its chemical compositions were detected. Since these layers contain a high volume of carbon agent, the amount of carbon content reported in EDX analysis (Figure 8) will be higher than titanium ones. The other conclusion is related to the high performance of MQL method. The created lubricant layers on the work part surface show that MQL technique is an ideal approach to deliver the lubricants to the cutting zone. The formed layer of lubricant is presented in Figure 4(c).

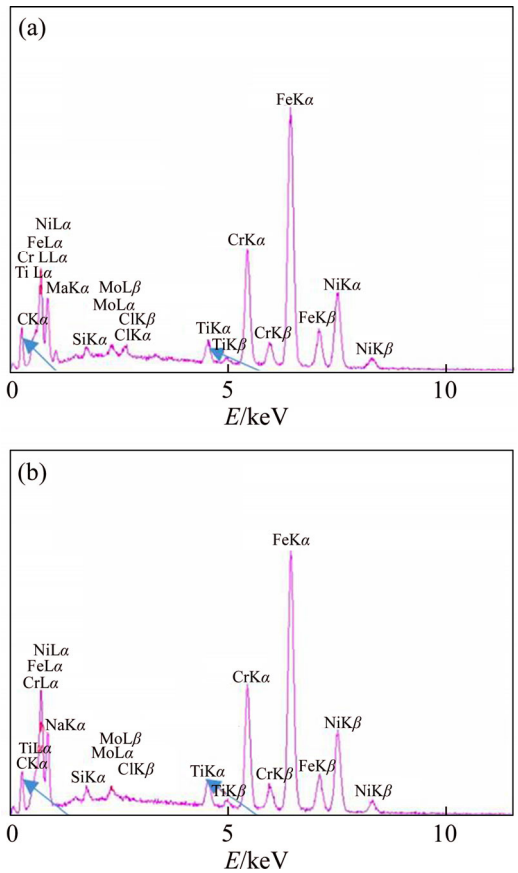

Figure 8 EDX analysis of work part surface (a) and adhered materials (b)

It is well known that the performance and product quality directly depend on the surface integrity induced from the last process. Surface integrity attributes are mainly grouped as mechanical, metallurgical and topological parameters (i.e., surface quality and other topological properties) of the work part [9]. Surface integrity is an important element when dealing with processes with high mechanical and thermal loads [1]. Therefore, R_a was studied as a criterion of surface integrity. Figure 9 presents the SEM image of the work part surface after MQL machining with two types of cutting fluids, including nanofluid with surfactant and conventional cutting fluid. The prepared surfaces have the closest values of R_a. Although these surfaces have similar levels of R_a, their surface qualities are not similar.

This phenomenon shows the necessity of studying factors governing surface quality improvement in the machining process. The removed zone on the work part surface under the use of conventional cutting fluid indicates that the machining process was conducted with no proper cutting mechanism. In other words, due to inappropriate lubrication and cooling performance of conventional cutting fluid and high machining temperature, the sharpness of cutting tool edge is lost rapidly, and the work part materials (chip) are removed under pushing mechanisms. In the other words, rubbing took place rather than adequate cutting process. Under these circumstances, generation of a surface with a high volume of the removed zone is not an unexpected phenomenon. However, using nanofluid tends to improve the lubrication conditions, and the high-quality machined surface is achieved.

Figure 10 represents the SEM images of the tool rake face under MQL machining with different cutting speed and conventional cutting fluid. As shown in Figure 10(c), the rounded edge cutting tool was used under cutting speed 95 m/min. Consequently, high abrasion wear was resulted. In addition, as shown in Figure 10(c), the presence of micro breakages on the cutting edge may also lead to tool failure when cutting process continues. Micro BUE as observed on the tool rake face of

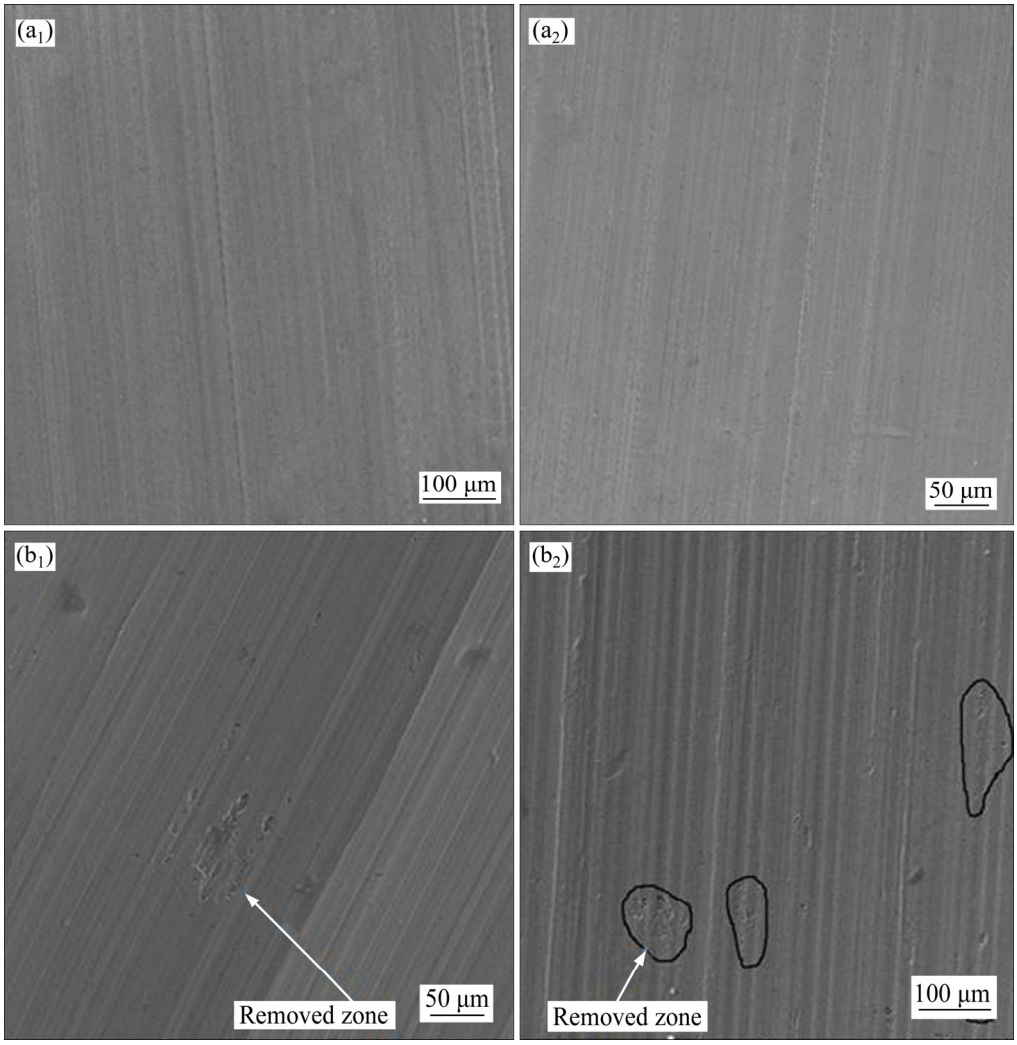

Figure 9 SEM image of machined work part surface when turning by nanofluid with surfactant and conventional cutting fluid: (a) NFS; (b) CF

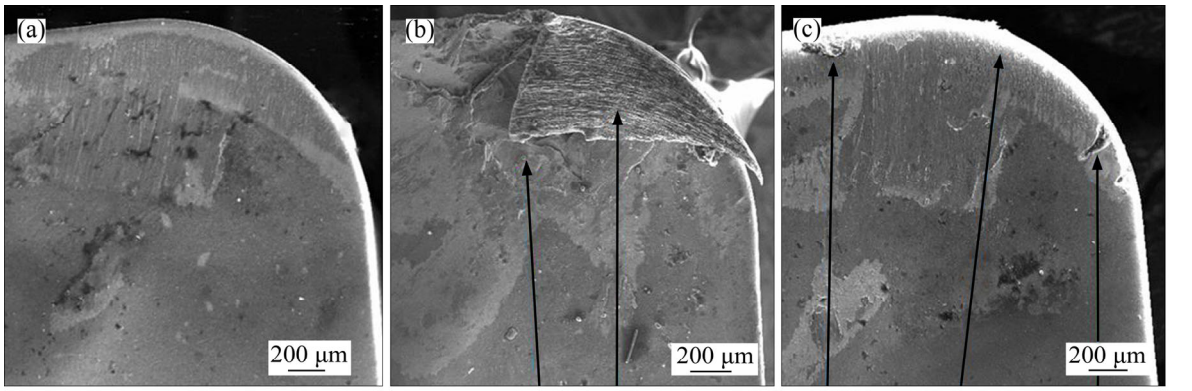

Figure 10 SEM images of tool rake face under different cutting speeds: (a) 45 m/min; (b) 70 m/min; (c) 95 m/min

Figure 10(c) can be clearly seen in Figures 11(a) and (b). Enlarged SEM images of micro breakage as well as tool failure when using the cutting speed of 95 m/min are presented in Figures 11(c) and (d), respectively.

Figure 12(a) shows the SEM image of detached particles on the tool rake face. Knowing that welded region of the work part materials with the cutting tool has a very high strength as compared with cutting tool materials, the increased

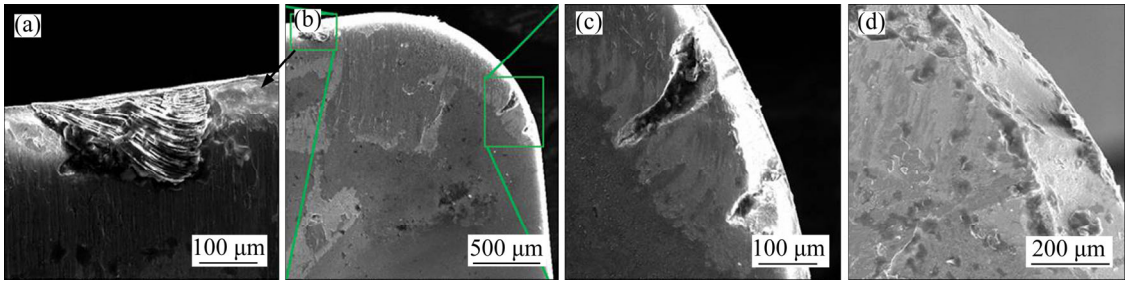

Figure 11 SEM images of tool rake face when using cutting speed of 95 m/min: (a) Micro BUE; (b) Tool rake face; (c) Micro breakage; (d) Failure

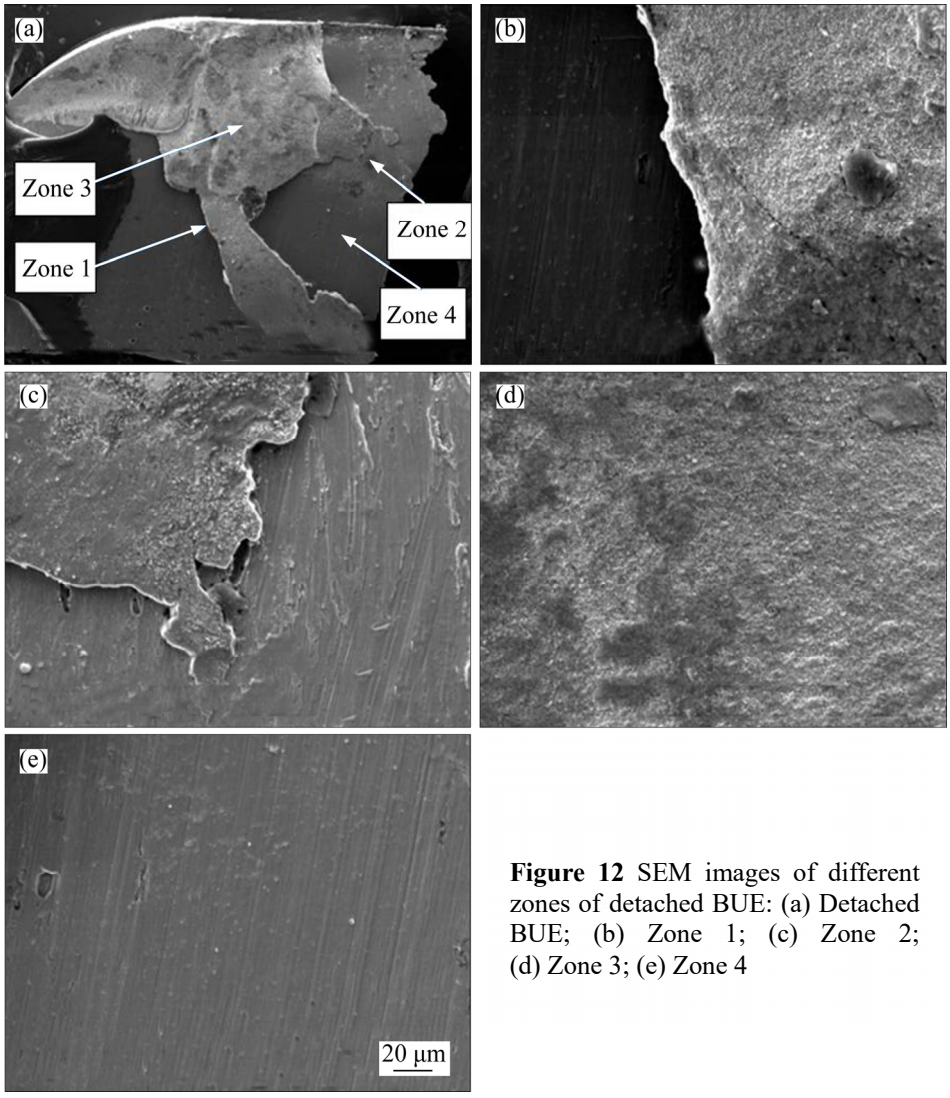

Figure 12 SEM images of different zones of detached BUE: (a) Detached BUE; (b) Zone 1; (c) Zone 2; (d) Zone 3; (e) Zone 4

cutting force may tend to remove the attached particles from tool rake face. Under such circumstance, a large region of tool rake face is destroyed. Figure 12 represents the SEM images of the other detached surfaces of BUE. These zones consist of a common area of tool and materials (zone 1 and zone 2), the removed surface of the cutting tool (zone 3), and the lower surface of detached BUE (zone 4).

To determine the residual particles on the tool rake face and chip surface which seem to be resulted from adhesion, the EDX mapping from removed chip was prepared. As shown in Figure 12(a), a significant broken area can be seen on the tool rake face. Therefore, the chemical analysis is encouraged to realize the chemical

composition of different zones that were defined in Figure 12. As shown in Figure 13, the EDX mapping analysis of the zone 1 shows that the dominant elements region 1 and region 2 were iron and tungsten, respectively. It proves the significant adhesion of the work part materials occurred on the tool rake face when conventional cutting fluid (or nanofluid without surfactant) was used.

The corresponding EDX map of the chip surface cutting tool in Figure 13(c) reveals the distribution of the tungsten, which is the primary element of the cutting tool. The presence of cutting tool elements on the detached area reveals that adhesion wear is the dominant mechanism. White points in Figure 13(a) indicate that iron element distribution is the main element of the A286 superalloy. In order to examine the chemical analysis of the noted surfaces (regions 1 and 2 in Figure 13(a)), the complete EDX map analysis was conducted. Figures 14 and 15 show the EDX map analysis for zone 3 and zone 4 in Figure 12. The presence of tungsten elements in chemical compositions of chip materials can be subjected to additional investigations. Referring to Table 1 (chemical compositions of A286) and EDX map analysis in Figure 14, it can be interpreted that the diffusion at high temperature (cutting zone temperature) leads to transferring the tungsten elements from cutting tool to the chip surface. On the other hand, the generated high temperature in machining superalloy intensifies the diffusion phenomenon, and consequently, lack of tungsten in cutting tool occurs. Under such circumstance, detached zone on the tool rake face quickly grows.

Figure 16 shows the SEM image as well as EDX mapping analysis of tool rake face with severe abrasion mechanism. The cutting tool presented in Figure 16 was used in a relatively long machining time with nanofluid with a surfactant. According to EDX analysis, the presence of iron, chrome, and nickel indicate that the presence of work part material in the wear region, although non-significant BUE or BUL was observed. Therefore, according to Figure 16, it can be exhibited that abrasion is the dominant wear mechanism. A comparative study of Figure 16 reveals the destructive effects of adhesion than abrasion.

4 Conclusions

Considering that A286 iron-based superalloy is known as a difficult-to-cut material, the appropriate machining and cooling schemes to improve the machining performance of A286 from different perspectives have received very low attention in the literature. Therefore, the proper selection of cutting fluid in precision machining of A286 is the first step for both industrial and academic sectors. Thus,

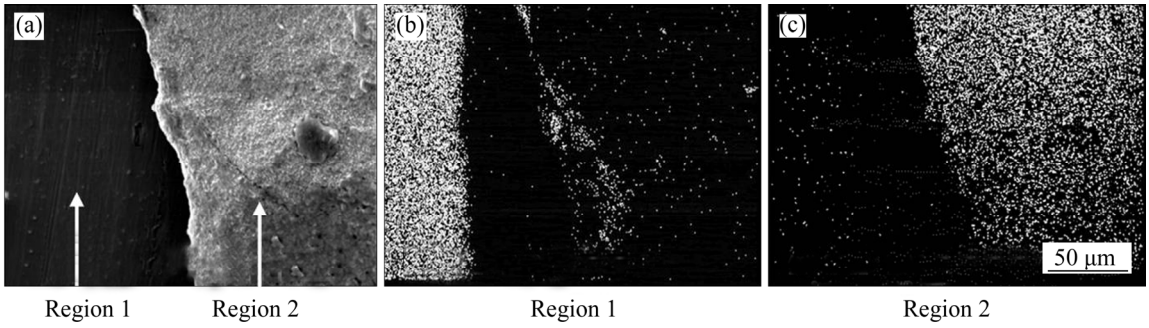

Figure 13 SEM images of zone 1 (a) and its elements map (b, c)

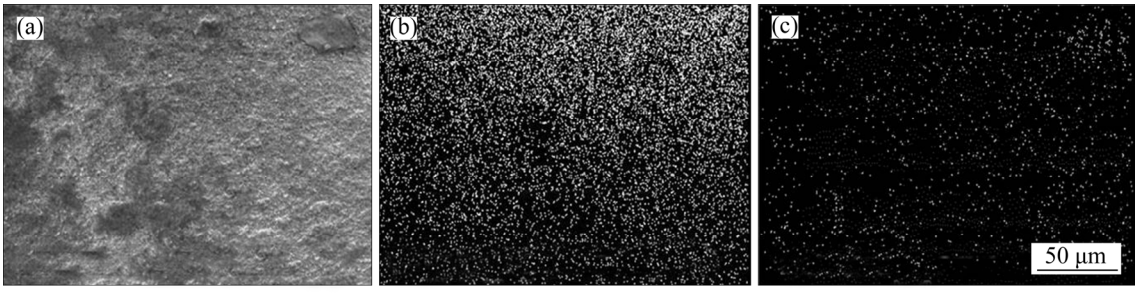

Figure 14 SEM image of zone 3 (a) and its elements map of tungsten (b) and carbon (c)

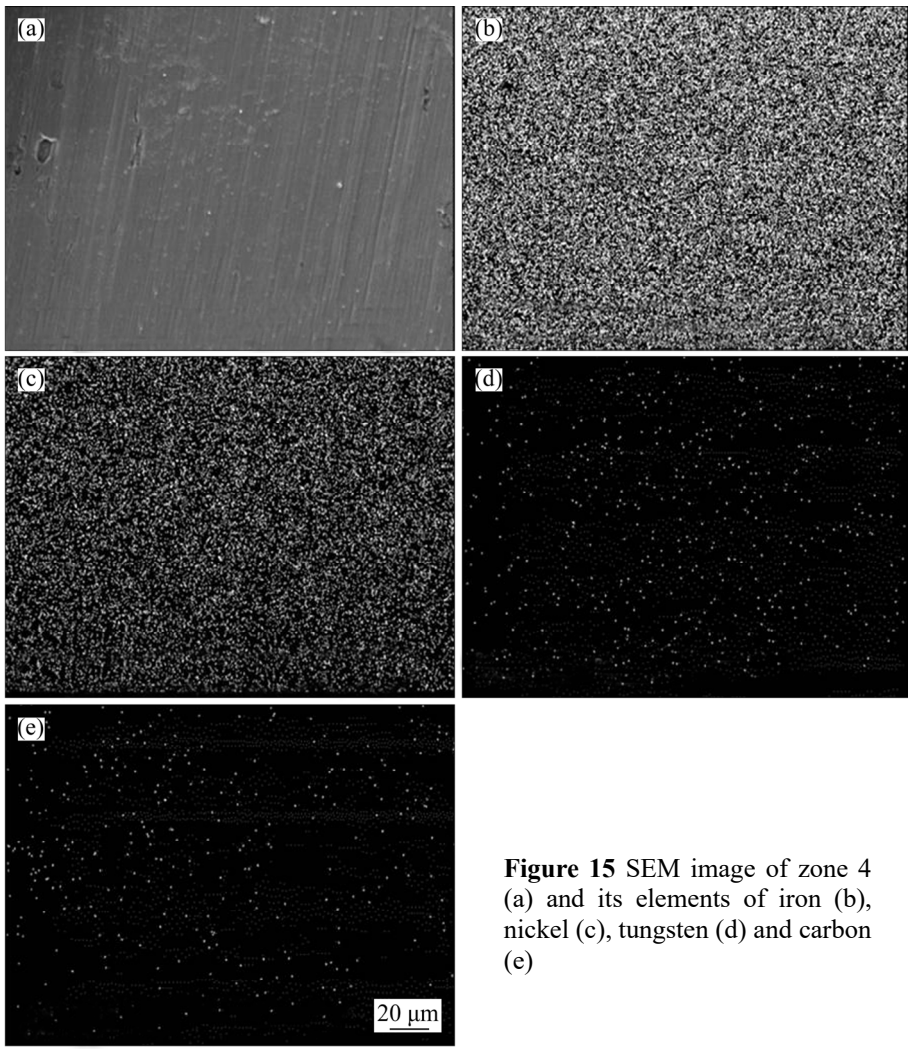

Figure 15 SEM image of zone 4 (a) and its elements of iron (b), nickel (c), tungsten (d) and carbon (e)

several turning tests on A286 work parts were conducted, and the effects of three modes of lubricants, conventional cutting fluid, nanofluid without surfactant (with copper-oxide and silicon-oxide nanoparticles), as well as nanofluid with surfactant (with copper-oxide and silicon-oxide nanoparticles) were studied on the tool wear morphologies of the machined parts. The main conclusions of this study are as follows:

1) The surfactant has significant effects on the stability of dispersed nanoparticles in nanofluid solution. Machining performance after 2 h of preparation of the nanofluid solution indicated that the absence of surfactant in nanofluid tends to change the nanofluid to conventional cutting fluid.

2) According to experimental characterizations with SEM and EDX approaches, the adhesion was observed as the dominant wear mechanism in turning A286. The BUE and BUL resulted from adhesion wear morphology may tend to rapid tool failure, if not controlled adequately. No similar defect was observed in the case of using nanofluid with a surfactant. Other mechanisms of tool wear such as severe abrasion and breakage were found in the case of using conventional cutting fluid and nanofluid without surfactant (after 2 h of nanofluid preparation). Whereas the wear mechanisms aforementioned did not occur when using nanofluid with surfactant.

3) Very high quality of the machined surface was observed when using nanofluid with surfactant. Contrary, the use of conventional cutting fluid or nanofluid without surfactant led to machined surfaces with several hindering problems such as adhered materials, removed zones as well as scratch.

4) The presence of tungsten agents in EDX map from chip surface resembles the presence of diffusion. Intensified diffusion may occur when temperature between two surfaces increases.

According to the EDX map and SEM images, in the absence of surfactant, the number of tungsten agents on-chip underneath the surface was increased. Therefore, it can be concluded that the use of surfactant led to less diffusion and consequently decreased adhesion wear on the cutting tool.

5) The SEM image of the tool flank face when BUE was detached from tool rake face showed high breakage on the cutting edge. This phenomenon led to catastrophic failure of the cutting tool; consequently, reduced tool life and work part surface quality are expected. Using nanoparticles with surfactant in the present study led to better control of this defect.

6) On the basis of SEM images of the flank face, it can be exhibited that the use of surfactant in nanofluid could change the wear mode from adhesion to abrasion. Consequently, better tool life is expected in the machining of A286 superalloy if the lower presence of adhesion is accomplished.

7) According to experimental observations, adhesion has more destructive effects on the iron-nickel based alloy than that observed from abrasion mode. Therefore, the use of adequate cooling strategies and cutting fluids is strongly advised in the case of high precision machining of iron-nickel based alloy where high quality and precision are demanded.

8) Additional investigations should be conducted on different surfactant including anionic, cationic, nonionic, and amphoteric. In addition, several models such as zeta potential of nanoparticles or turbidity measurement by spectrophotometer can be used to study nanoparticles stability.

References

[1] THAKUR A, GANGOPADHYAY S. State-of-the-art in surface integrity in machining of nickel-based superalloys [J]. International Journal of Machine Tools & Manufacture, 2016, 100: 25–54.

[2] SARIKAYA M, YILMAZ V, GÜLLÜ A. Analysis of cutting parameters and cooling/lubrication methods for sustainable machining in turning of Haynes 25 superalloy [J]. Journal of Cleaner Production, 2016, 133: 172–181.

[3] ULUTAN D, OZEL T. Machining induced surface integrity in titanium and nickel alloys: A review [J]. International Journal of Machine Tools & Manufacture, 2011, 51: 250–280.

[4] ZHANG S, LI J F, WANG Y W. Tool life and cutting forces in end milling Inconel 718 under dry and minimum quantity cooling lubrication cutting conditions [J]. Journal of Cleaner Production, 2012, 32: 81–87.

[5] TAZEHKANDI A H, PILEHVARIAN F, DAVOODI B. Experimental investigation on removing cutting fluid from turning of Inconel 725 with coated carbide tools [J]. Journal of Cleaner Production, 2014, 80: 271–281.

[6] GUO C B, WEI D B, DI S C. Improving energy utilization efficiency of electrical discharge milling in titanium alloys machining [J]. Journal of Central South University, 2016, 23: 2550–2557.

[7] CHEN H, CHEN K H, XU Y C, PAN C X, YI J Y, ZHU C J. Microstructure, mechanical properties, and milling performance of arc-PVD AlTiN-Cu and AlTiN/AlTiN-Cu coatings [J]. Journal of Central South University, 2018, 25: 506–515.

[8] ZHANG Y J, DONG G J, ZHOU M. Simulation and experiment analysis on thermal deformation of tool system in single-point diamond turning of aluminum alloy [J]. Journal of Central South University, 2016, 23: 2223–2229.

[9] SHOKRANI A, DHOKIA V, NEWMAN S T. Environmentally conscious machining of difficult-to-machine materials with regard to cutting fluids [J]. International Journal of Machine Tools & Manufacture, 2012, 57: 83–101.

[10] CHETAN, BEHER B C, GHOSH A S, RAO P V. Wear behavior of PVD TiN coated carbide inserts during machining of Nimonic 90 and Ti6Al4V superalloys under dry and MQL conditions [J]. Ceramics International, 2016, 42: 14873–14885.

[11] DAVOODI B, ESKANDARI B. Tool wear mechanisms and multi-response optimization of tool life and volume of material removed in turning of N-155 iron-nickel-base superalloy using RSM [J]. Measurement, 2015, 68: 286–294.

[12] CHENG Q, REN W D, LIU Z F, CHEN D J, GU P H, Load-induced error identification of hydrostatic turntable and its influence on machining accuracy [J]. Journal of Central South University, 2016, 23: 2558–2569.

[13] CUI W, TANG J Y. New method for calculating face gear tooth surface involving worm wheel installation errors [J]. Journal of Central South University, 2017, 24: 1767–1778.

[14] POLVOROSA R, SUAREZ A, LOPEZ de LACALLE L N, CERRILLO I, WRETLAND A, VEIGA F. Tool wear on nickel alloys with different coolant pressures: Comparison of alloy 718 and Waspaloy [J]. Journal of Manufacturing Processes, 2017, 26: 44–56.

[15] WANG Q B, MA H B, KONG X G, ZHANG Y M, A distributed dynamic mesh model of a helical gear pair with tooth profile errors [J]. Journal of Central South University, 2018, 25: 287–303.

[16] FANG Z H, OBIKAWA T. Turning of Inconel 718 using inserts with cooling channels under high pressure jet coolant assistance [J]. Journal of Materials Processing Technology 2017, 247: 19–28.

[17] CANTERO J L, ALVAREZ J D, MIGUELEZ M H, MARIN N C. Analysis of tool wear patterns in finishing turning of Inconel 718 [J]. Wear, 2013, 297: 885–894.

[18] HOIER P H, KLEMENT U, ALAGAN N T, BENO T, WRETLAND A. Flank wear characteristics of WC-Co tools when turning Alloy 718 with high-pressure coolant supply [J]. Journal of Manufacturing Processes, 2017, 30: 116–123.

[19] LIMA F F, SALES W F, COSTA E S, FLÁVIO J da SILVA, MACHADO A R. Wear of ceramic tools when machining Inconel 751 using argon and oxygen as lubri-cooling atmospheres [J]. Ceramics International, 2016, 43: 667–685.

[20] BEHERA C H, ALEMAYEHU H, GHOSH S, RAO P V. A comparative study of recent lubri-coolant strategies for turning of Ni-based superalloy [J]. Journal of Manufacturing Processes, 2017, 30: 541–552.

[21] TAZEHKANDI A H, SHABGARD M, PILEHVARIAN F. Application of liquid nitrogen and spray mode of biodegradable vegetable cutting fluid with compressed air in order to reduce cutting fluid consumption in turning Inconel 740 [J]. Journal of Cleaner Production, 2015, 108: 90–103.

[22] GRZESIK W, NIESLONY P, HABRAT W, SIENIAWSKI J, LASKOWSKI P. Investigation of tool wear in the turning of Inconel 718 superalloy in terms of process performance and productivity enhancement [J]. Tribology International, 2017, 118: 337–346.

[23] ISRAEL M, RYUTARO T, YASUO Y, KATSUHIKO S, KEIJI Y, SYUHEI Y, MITSURU H. Effect of coating layer loss on the wear rate change of coated carbide tools in turning process [J]. Precision Engineering, 2017, 50: 1–7.

[24] CALISKAN H, KUCUKKOSE M. The effect of aCN/TiAlN coating on tool wear, cutting force, surface finish and chip morphology in face milling of Ti6Al4V superalloy [J]. International Journal of Refractory Metals and Hard Materials, 2015, 50: 304–312.

[25] NIAKI F A, MEARS L. A comprehensive study on the effects of tool wear on surface roughness, dimensional integrity and residual stress in turning IN718 hard-to-machine alloy [J]. Journal of Manufacturing Processes, 2017, 30: 268–280.

[26] KOSEKI S H, INOUE K, MORITO S H, OHBA T, USUKI H. Comparison of TiN-coated tools using CVD and PVD processes during continuous cutting of Ni-based superalloys [J]. Surface & Coatings Technology, 2015, 283: 353–363.

[27] SUGIHARA T, NISHIMOTO Y, ENOMOTO T. Development of a novel cubic boron nitride cutting tool with atextured flank face for high-speed machining of Inconel 718 [J]. Precision Engineering, 2017, 48: 75–82.

[28] FANG Z, OBIKAWA T. Cooling performance of micro-texture at the tool flank face under high pressure jet coolant assistance [J]. Precision Engineering, 2017, 49: 41–51.

[29] CHOI S U S, EASTMAN J A. Enhancing thermal conductivity of fluids with nanoparticles [J]. ASME Fed, 1995, 231: 99–105.

[30] SIDIK N A, SAMION S, GHADERIAN J, YAZID M N. Recent progress on the application of nanofluids in minimum quantity lubrication machining: A review [J]. International Journal of Heat and Mass Transfer, 2017, 108: 79–89.

[31] CHETAN, BEHERA B C, GHOSH S, RAO P V. Application of nanofluids during minimum quantity lubrication: A case study in turning process [J]. Tribiology International, 2016, 101: 234–246.

[32] GUPTA M K, SOOD P K, SHARMA V S. Optimization of machining parameters and cutting fluids during nano-fluid based minimum quantity lubrication turning of titanium alloy by using evolutionary techniques [J]. Journal of Cleaner Production, 2016, 135: 1276–1288.

[33] PADMINI R, VAMSI KRISHNA P, KRISHNA MOHANA RAO G. Effectiveness of vegetable oil based nanofluids as potential cutting fluids in turning AISI 1040 steel [J]. Tribology International, 2016, 94: 490–501.

[34] NAJIHA M S, RAHMAN M M, KADIRGAMA K. Performance of water-based TiO_2 nanofluid during the minimum quantity lubrication machining of aluminum alloy, AA6061-T6 [J]. Journal of Cleaner Production, 2016, 135: 1623–1636.

[35] LIU Z H, AN Q, XU J, CHEN M, HAN S H. Wear performance of (nc-AlTiN)/(a-Si_3N_4) coating and (nc-AlCrN)/(a-Si3N4) coating in high speed machining of titanium alloys under dry and minimum quantity lubrication (MQL) conditions [J]. Wear, 2013, 305: 249–259.

[36] SARTORI S, GHIOTTI A, BRUSCHI S. Hybrid lubricating/cooling strategies to reduce the tool wear in finishing turning of difficult-to-cut alloys [J]. Wear, 2017, 376–377: 107–114.

[37] GUO J, BARBER G C, SCHALL D J, ZOU Q, JACOB S B. Tribological properties of ZnO and WS_2 nanofluids using different surfactants [J]. Wear, 2017, 382–383: 8–14.

[38] XIA W, ZHAO J, CHENG X, SUN J, WU H, YAN Y, JIAO S, JIANG Z. Study on growth behaviour of oxide scale and its effects on tribological property of nano-TiO_2 additive oil-in-water lubricant [J]. Wear, 2017, 376–377: 792–802.

[39] SHARMA K, TIWARI A K, DIXIT A R, SINGH R K, SINGH M. Novel uses of alumina/graphene hybrid nanoparticle additives for improved tribological properties of lubricant in turning operation [J]. Tribology International, 2018, 119: 99–111.

[40] BORDIN A, BRUSCHI S, GHIOTTI A, BARIANI P F. Analysis of tool wear in cryogenic machining of additive manufactured Ti6Al4V alloy [J]. Wear, 2015, 328–329: 89–99.

[41] ASLANTAS K, UCUN İ, ÇICEK A. Tool life and wear mechanism of coated and uncoated Al_2O_3/TiCN mixed ceramic tools in turning hardened alloy steel [J]. Wear, 2012, 274–275: 442–451.

[42] GOMEZ-PARRA A, ALVAREZ-ALCON M, SALGUERO J, BATISTA M, MARCOS M. Analysis of the evolution of the built-up edge and built-up layer formation mechanisms in the dry turning of aeronautical aluminium alloys [J]. Wear, 2013, 302: 1209–1218.

[43] MUSAVI S H, DAVOODI B, NIKNAM S A. Environmental-friendly turning of A286 superalloy [J]. Journal of Manufacturing Processes, 2018, 32: 734–743.

[44] CORREA J G, SCHROETER R B, MACHADO A R. Tool life and wear mechanism analysis of carbide tools used in the machining of martensitic and super martensitic stainless steels [J]. Tribology International, 2017, 105: 102–117.

(Edited by YANG Hua)

中文导读

纳米颗粒增强纳米流体对刀具磨损形貌的影响

摘要：高温合金属于硬切削材料，加工性较差。在高温合金加工，刀具磨损被认为是切削性能的主要特征之一。虽然关于高温合金加工过程中影响刀具寿命的因素已有大量报道，但关于纳米粒子稳定性对纳米流体性能的影响以及由此导致的刀具磨损形貌的研究尚未见报道。在本工作中，通过提高基液的稳定性来增强纳米粒子。在此基础上，将切削液中加入表面活性剂作为增强剂，研究新型润滑剂对A286 工件刀具磨损形貌的影响。

关键词：纳米流体；表面活性剂；纳米粒子分散；堆积边缘